JOURNAL OF SOLID STATE CHEMISTRY 64, 347–358 (1986)

Synthesis and Structure of Ternary Molybdenum Oxides $M Mo_8O_{10}$ (M = Li or Zn) Having Orthogonal Nonintersecting Octahedral Cluster Chains*,†

KWANG-HWA LII, ROBERT E. McCARLEY,‡ SANGSOO KIM, AND ROBERT A. JACOBSON

Ames Laboratory, USDOE and Department of Chemistry, Iowa State University, Ames, Iowa 50011

Received November 30, 1985

The new compounds $LiMo_8O_{10}$ (**I**) and $ZnMo_8O_{10}$ (**II**) have been prepared via reactions in sealed Mo-tubes at 1370–1450°C between Li_2MoO_4, MoO_3, and Mo (3 : 16 : 29 mole ratio), and ZnO, MoO_3, and Mo (1 : 3 : 5 mole ratio), respectively. The isomorphous compounds are tetragonal, space group $I4_1md$, $Z = 4$, with lattice constants $a = 5.8515(6)$ Å, $c = 24.783(3)$ Å for **I**, and $a = 5.8961(4)$ Å, $c = 24.840(3)$ Å for **II**, as determined from Guinier X-ray powder patterns. Single crystal structure determination shows that these compounds are constructed from infinite chains consisting of edge-shared octahedral cluster units. The structure can be viewed as a stacking along the c axis of layers consisting of parallel chains, with the chains in successive layers oriented alternately along the a and b axes. Intra- and interlayer crosslinking of the chains by Mo—O—Mo bonds is represented in the connective formula $[(Mo_2Mo_{4/2}O_{6/2}O_{4/3})O_{2/3}]$ for the octahedral cluster subunits. Mo—Mo bonding within the subunits is strong, but very irregular compared to analogous compounds containing such chains. Subunit Mo—Mo bond order sums indicate that the bond distortions are effective in accommodating a higher electron count in metal–metal bonding states. It is shown that the structures are related to the spinel and rock salt structures through an ordered-defect arrangement of the Mo and O atoms.

Introduction

There are now known several structure types, typified by $NaMo_4O_6$ (*1*), $Sc_{0.75}Zn_{1.25}Mo_4O_7$ (*2*), $Mn_{1.5}Mo_8O_{11}$ (*3*), and $Ca_{5.45}Mo_{18}O_{32}$ (*4*), which contain infinite chains of octahedral cluster units fused on opposite (*trans*) edges. The chains can be regarded as being formed from condensation of M_6X_{12} cluster units (*5*) by elimination of two X atoms bridging *trans* edges of the M_6 octahedral cluster unit and sharing of both M and X atoms between adjacent units along the chain, as indicated by the connective formula $Na[(Mo_2Mo_{4/2}O_{8/2}O_{2/2})O_{2/2}]$ for $NaMo_4O_6$. In each of the above structure types the infinite chains are extended along one crystallographic

* Presented at the Symposium on Synthesis in Solid State Chemistry: Frontier Structures and Novel Results, held during the American Chemical Society Meeting, Chicago, Ill., September 9–11, 1985.

† This work was supported by the U.S. Department of Energy through the Ames Laboratory, which is operated by Iowa State University under Contract W-7405-Eng-82. This research was supported by the Director of Energy Research, Office of Basic Energy Sciences.

‡ To whom correspondence should be addressed.

0022-4596/86 $3.00

axis to produce a material having pseudo-one-dimensional character. Coupling of the infinite chains through Mo—O—Mo crosslinking creates channels in which the ternary metal ions are located in sites surrounded by O atoms arranged in coordination polyhedra of various geometries.

Essential elements for formation of cluster units and their condensation to form infinite chains are reduction of the metal atoms to provide electrons for metal–metal bonding, and lowering of the *X/M* ratio to promote unhindered close approach of the metal atoms and formation of strong *M—M* bonds (*5, 6*). Progressive reduction should lead from discrete cluster compounds, e.g., $M_nMo_3O_8$ (*7*) and $M_nMo_8O_{16}$ (*8, 9*), to infinite chains, e.g., $Ca_{5.45}Mo_{18}O_{32}$ (*4*) and $Na_2Mo_4O_6$ (*1*), and ultimately to structures condensed in three dimensions, like $NbO(Nb_{6/2}O_{12/4})$ (*10*) and the metal itself. A logical result included as an intermediate step of this progression is formation of compounds having infinite chains extended in two directions. A few compounds having such structures are known, e.g., $NaPt_3O_4$ (*11*), $CaPt_2O_4$ (*12*), and $Hg_{2.86}AsF_6$ (*13*). We report here the synthesis and structures of $LiMo_8O_{10}$ and $ZnMo_8O_{10}$, which constitute the first members with orthogonal, nonintersecting chains consisting of edge-fused octahedral cluster units.

Synthesis

$LiMo_8O_{10}$. Small chunky crystals of this compound were first discovered in a product mixture resulting from the reaction of Li_2MoO_4, MoO_3, and Mo in a 3 : 8 : 13 mole ratio in a sealed Mo-tube at 1450°C for 1.5*d*. The composition of a crystal of this new compound, chosen from the product mixture, was established through subsequent X-ray structure determination. An essentially pure product was then prepared by heating a pressed pellet containing the required amounts of powdered Li_2MoO_4, MoO_3, and Mo (3 : 16 : 29 mole ratio) in a sealed Mo-tube at 1410°C for 2*d*. A Guinier X-ray powder pattern faintly showed the strongest line of Mo metal, but all other lines in the powder pattern could be indexed on the structure of $LiMo_8O_{10}$. This compound appears to be unreactive toward air and water over a period of at least a few hours.

$ZnMo_8O_{10}$. The appropriate quantities of powdered ZnO, MoO_3, and Mo (1 : 3 : 5 mole ratio) were mixed, pelletized, and heated in a sealed Mo-tube at 1370°C for 2*d*. An X-ray powder pattern showed only the strongest line of Mo metal in addition to the lines which could be indexed on the structure of $ZnMo_8O_{10}$. A reaction performed at lower temperature (1250°C) for 65 hr resulted in a mixture containing $ZnMo_8O_{10}$, $Zn_2Mo_3O_8$, MoO_2, and Mo.

Other compounds. Attempts to prepare other compounds with the composition MMo_8O_{10} (*M* = Mg, Fe, Co, Ni, and Si) were unsuccessful. Reaction conditions and observed products are summarized as follows.

$MgMo_8O_{10}$ (MgO, MoO_3, Mo, 1410°C, 2 days), MoO_2, Mo, and $Mg_2Mo_3O_8$. Fe Mo_8O_{10} (Fe_2O_3, MoO_3, Mo, 1400°C, 42 hr), MoO_2, Mo, and $Fe_{1.89}Mo_{4.11}O_7$. $SiMo_8O_{10}$ (Si, MoO_3, Mo, 1630°C, 2 days), Mo, SiO_2 (JCPDS 11-695). $CoMo_8O_{10}$ (CoO, MoO_3, Mo, 1375°C, 3 days), MoO_2, Mo. $NiMo_8O_{10}$ (NiO, MoO_3, Mo, 1375°C, 3 days), MoO_2, Mo, α-$NiMoO_4$.

Preliminary Film Work and X-Ray Powder Diffraction

A single crystal of the lithium compound in the form of a chunk was mounted on a Weissenberg camera with the *a* axis parallel to the rotation axis. Oscillation and 0*kl*-1*kl* layer photographs were registered. The Weissenberg photographs suggested that the Laue group was 4/*mmm* with the rough unit cell parameters $a = b = 5.88$ Å, $c =$

24.7 Å. Systematic absences were observed for *hkl* with $h + k + l = 2n$ and *hhl* with $2h + l = 4n$.

The film work on a single crystal of Zn Mo_8O_{10} indicated that it was isomorphous with $LiMo_8O_{10}$. The unit cell parameters which were calculated from the axial oscillation and Weissenberg photographs were $a = b = 5.90$ Å, $c = 24.9$ Å.

The Guinier powder patterns of both compounds could be completely indexed on the basis of body-centered tetragonal cells with $a = b = 5.8515(6)$ Å, $c = 24.783(3)$ Å for $LiMo_8O_{10}$, and $a = b = 5.8961(4)$ Å, $c = 24.840(3)$ Å for $ZnMo_8O_{10}$. Cell constants derived from the Guinier powder diffraction were used in later calculations because of their high accuracy.

Because $ZnMo_8O_{10}$ showed a phase transition in the magnetic susceptibility data (*14*) a low-temperature (100–110 K) X-ray powder pattern was taken below the transition temperature (ca. 200 K) with a Rigaku powder diffractometer. NBS Si powder was mixed with the sample as an internal standard. Both R.T. and L.T. powder patterns were taken under the same conditions for data collection. $CuK\alpha_1$ ($\lambda = 1.54056$ Å) was used for calculating the unit cell parameters. The cell constants calculated from these R.T. and L.T. powder patterns are $a = b = 5.9003(4)$ Å, $c = 24.848(2)$ Å, and $a = b = 5.896(1)$ Å, $c = 24.836(5)$ Å, respectively. No extra reflections were detected at 100 K. Although the intensities of a few diffraction peaks appear different at low temperature, atomic positions obtained from single crystal X-ray diffraction data collected at 160 K did not show any significant differences from those obtained using the room-temperature data.

X-Ray Single Crystal Diffraction Studies

The crystals were transferred to four-circle diffractometers and were centered. The preliminary unit cell constants and orientation matrices were determined by using an automatic indexing program (*15*) that uses reflections from ω-oscillation pictures as input. Crystal data and details of the parameters associated with data collection for both compounds are tabulated in Table I. Corrections for absorption effects were based on ϕ scans of suitable reflections with χ values close to 90°. Lorentz and polarization corrections were also applied. Both data sets showed $4/mmm$ Laue symmetry and the extinction conditions $h + k + l = 2n$ for *hkl* reflections, and $2h + l = 4n$ for *hhl* reflections. The possible space groups thus were $I4_1md$ (No. 109), and $I\bar{4}2d$ (No. 122). The structures can be better described in space group $I4_1md$ (vide infra). The atomic scattering factors (*16*) for neutral atoms were used throughout the calculations. Both real and imaginary components of anomalous dispersion (*17*) were included for all atoms heavier than oxygen. The data sets were averaged in $4/mmm$ symmetry without any reflections being eliminated.

Structure solution of $LiMo_8O_{10}$. Initial attempts to solve this structure using either direct methods (MULTAN80) or Patterson Harker analysis were unsuccessful. The Patterson function was found to contain many overlapped peaks which prevented structural solution. Patterson superposition analyses were next employed using a variety of shift vectors, initially without success, until an isolated vector which appeared to be a Mo—O vector was selected for a weighted superposition. The top 40 peaks that resulted clearly revealed the crystal structure. Subsequent refinement, however, indicated that no oxygen atom existed at the position corresponding to the head of the shift vector; instead a relatively large "ripple" arising from termination effects occupied this position. Since the Patterson function merely represents a self-convolution of the electron density function, even such a ripple can image the structure. This is the first example to our

TABLE 1

CRYSTALLOGRAPHIC DATA FOR $LiMo_8O_{10}$ AND $ZnMo_8O_{10}$

	$LiMo_8O_{10}$	$ZnMo_8O_{10}$
Crystal system	Tetragonal	Tetragonal
Space group	$I4_1md$	$I4_1md$
Lattice constants (Å)		
a	5.8515(6)	5.8961(4)
c	24.783(3)	24.840(3)
Volume (Å^3)	848.6(2)	863.5(1)
Z	4	4
Density (calcd) (g/cm^3)	7.317	7.640
Crystal dimensions (mm)	0.2 × 0.14 × 0.08	0.30 × 0.14 × 0.08
Abs. coeff. (cm^{-1})	112.1	137.8
Reflections for absorp. corr.		
(hkl, 2θ, T_{max}/T_{min})	040, 28.08, 2.06	600, 42.38, 1.61 200, 13.84, 1.77
Radiation: Mo$K\alpha$ (λ, Å)	0.71034	0.70966
Scan type: ω-scan		
Monochromator: graphite		
Scan half-width (degree)	0.5	0.6
Standard reflections		
Number monitored	3	3
Frequency measured	Every 75 refins.	Every 50 refins.
Intensity variation	None	None
Reflections measured	hkl, $\bar{h}\,\bar{k}\,l$, $\bar{h}k\bar{l}$	hkl, $\bar{h}\,\bar{k}\,l$, $\bar{h}k\bar{l}$
Max. 2θ (degree)	60	62.5
Reflections collected	2356	2022
Observed [$I > 3\sigma(I)$]	2156	2001
Number unique refins. [$I > 3\sigma(I)$]	374	443
Number parameters refined	42	56
R (%)[a]	4.2	2.6
R_w (%)[b]	5.2	3.2
Quality of fit indicator[c]	1.94	1.315

[a] $R = \Sigma||F_o| - |F_c||/\Sigma|F_o|$.

[b] $R_w = [\Sigma w(|F_o| - |F_c|)^2]/\Sigma w|F_o|^2]^{1/2}$; $w = 1/\sigma^2(|F_o|)$.

[c] Quality of fit = $[\Sigma w(|F_o| - |F_c|)^2$ (N observations) − N(parameters))]$^{1/2}$.

knowledge where such a ripple effect has been used to aid in structure determination. We have subsequently verified this effect with a different structure and are now pursuing its general ramifications.

The position of all the oxygen atoms were revealed on a Fourier synthesis using phases from molybdenum atoms.[1] Inspec-

[1] Calculations were carried out on a VAX 11/780 computer. Structure factor calculations and least-squares refinement were done using the block matrix/full matrix program ALLS (R. L. Lapp and R. A. Jacobson, U.S. Department of Energy Report IS-4708, Iowa State University, Ames, Iowa, 1979), Fourier series calculations were done using the program FOUR (D. R. Powell and R. A. Jacobson, U.S. Department of Energy Report IS-4737, Iowa State University, Ames, Iowa, 1980), and for molecular drawings the program ORTEP (C. K. Johnson, U.S. Atomic Energy Commission Report ORNL-3794, Oak Ridge National Laboratory, Oak Ridge, Tenn., 1970) was used. An empirical absorption correction was carried out using diffractometer ϕ-scan data and the program ABSN (B. A. Karcher, Ph.D. dissertation, Iowa State University, 1981).

TABLE II

POSITIONAL PARAMETERS FOR LiMo$_8$O$_{10}$

Atom	Position	Multiplier	x	y	z	B^a (Å^2)
Mo1	8b	0.5	0.5	0.2262(2)	0.0	0.56
Mo2	8b	0.5	0.0	0.2353(3)	0.00429(6)	0.64
Mo3	8b	0.5	0.0	0.2480(3)	0.32808(7)	0.96
Mo4	8b	0.5	0.0	0.2760(2)	0.17549(6)	0.63
O1	8b	0.5	0.5	0.246(2)	0.250(1)	0.59
O2	8b	0.5	0.5	0.239(2)	0.0811(7)	0.48
O3	8b	0.5	0.5	0.230(2)	0.4224(9)	1.06
O4	8b	0.5	0.0	0.242(3)	0.085(1)	1.36
O5	8b	0.5	0.0	0.263(2)	0.4144(9)	0.24
Li	4a	0.25	0.5	0.5	0.131(2)	1.33

[a] The isotropic equivalent thermal parameter is defined as $B = 4/3 [a^2\beta_{11} + b^2\beta_{22} + c^2\beta_{33} + 2ab(\cos\gamma)\beta_{12} + 2ac(\cos\beta)\beta_{13} + 2bc(\cos\alpha)\beta_{23}]$.

tion of observed and calculated structure factors showed that some reflections were strongly affected by secondary extinction effect. A least-squares refinement with anisotropic thermal parameters on all molybdenum atoms and with an isotropic extinction factor yielded an agreement factor $R = 4.7\%$. A subsequent ΔF map clearly showed peaks at the 4*a* special position which were most likely due to lithium ions. A refinement including the multiplier for the lithium atom resulted in $m(\text{Li}) = 0.33(3)$ suggesting that the lithium site was probably fully occupied. Final refinement of all positional parameters, anisotropic thermal parameters for Mo atoms, isotropic thermal factors for oxygen and lithium atoms, and isotropic extinction factor led to convergence with $R = 4.2\%$ and $R_w = 5.2\%$. The oxygen atoms were isotropically refined because some of them gave negative thermal parameters when they were anisotropically varied. The secondary extinction parameter was 4.38×10^{-4}. A final difference-Fourier synthesis based on all data showed a maximum residual electron density of 1.1 e/Å^3 which is near the Mo1 site. The final positional and isotropic thermal parameters are collected in Table II. The selected bond distances and bond angles are given in Tables III and IV.

In order to ensure that the correct space group ($I4_1md$) had indeed been selected, refinement was also carried out in space group $I\bar{4}2d$. The former clearly resulted in significantly lower residual indices than the latter ($R = 15.4$, $R_w = 20.2\%$).

TABLE III

BOND DISTANCES (Å) FOR LiMo$_8$O$_{10}$

Mo1–Mo1	2.648(2)	Mo1–O1	2.153(9)
Mo1–Mo2	2.9282(3)	Mo1–O2	2.01(2)
Mo1–Mo3	2.757(2)	Mo1–O5	2.12(2)
Mo1–Mo4	2.788(2)	Mo2–O1	2.149(9)
Mo2–Mo2	2.754(3)	Mo2–O3	2.04(2)
Mo2–Mo3	2.723(2)	Mo2–O4	2.01(3)
Mo2–Mo4	2.725(2)	Mo3–O2	2.015(8)
Mo3–Mo3	2.950(3)	Mo3–O4	2.05(1)
	2.902(3)	Mo3–O5	2.14(2)
Mo4–Mo4	2.621(3)	Mo4–O3	2.05(1)
	3.230(3)	Mo4–O4	2.24(3)
Mo3–Mo4[a]	3.258(2)	Mo4–O5	2.147(9)
Mo1–Mo1[a]	3.204(2)	Li–O2	1.96(3)
Mo2–Mo2[a]	3.098(3)	Li–O3	1.70(3)

[a] Interchain distance.

TABLE IV

BOND ANGLES (DEGREE) FOR LiMo$_8$O$_{10}$[a]

Mo1–Mo1–Mo2	91.04(4)	O1–Mo1–O1	88.9(5)
Mo2–Mo1–Mo2	175.35(6)[b]	O1–Mo1–O2	88.4(8)
Mo1–Mo2–Mo2	88.96(4)	O1–Mo1–O5	88.7(8)
Mo4–Mo1–Mo1	61.64(3)	O2–Mo1–O5	176.2(5)
Mo4–Mo2–Mo2	59.65(3)	O1–Mo2–O1	87.5(5)
Mo3–Mo1–Mo1	61.30(3)	O1–Mo2–O3	83.1(8)
Mo3–Mo2–Mo2	59.62(3)	O1–Mo2–O4	92.0(8)
Mo4–Mo1–Mo2	56.89(4)	O3–Mo2–O4	173.2(6)
Mo3–Mo1–Mo2	57.14(4)	O2–Mo3–O2	87.8(5)
Mo1–O1–Mo2	85.77(5)	O2–Mo3–O4	92.0(4)
Mo2–O4–Mo4	176.1(9)	O2–Mo3–O4	172.8(9)
Mo3–O4–Mo4	98.6(9)	O2–Mo3–O5	89.6(5)
Mo1–O5–Mo3	179.4(7)	O4–Mo3–O4	87.3(7)
Mo3–O5–Mo4	98.9(7)	O4–Mo3–O5	83.2(8)
O2–Li–O2	103(2)	O3–Mo4–O3	100.5(5)
O2–Li–O3	112.4(4)	O3–Mo4–O4	91.1(7)
O3–Li–O3	105(2)	O3–Mo4–O5	88.8(4)
		O3–Mo4–O5	166.5(7)
		O4–Mo4–O5	78.8(7)
		O5–Mo4–O5	80.5(5)

[a] The atom labels refer to Fig. 2.

[b] This angle corresponds to the dihedral angle between basal planes of adjacent octahedra.

TABLE V

POSITIONAL PARAMETERS FOR $ZnMo_8O_{10}$

Atom	Position	Multiplier	x	y	z	B^a (Å^2)
Mo1	8b	0.5	0.5	0.2192(1)	0.0	0.23
Mo2	8b	0.5	0.0	0.2389(1)	0.00451(4)	0.25
Mo3	8b	0.5	0.0	0.2715(1)	0.32858(5)	0.22
Mo4	8b	0.5	0.0	0.2752(2)	0.17670(5)	0.22
O1	8b	0.5	0.5	0.244(2)	0.2538(7)	0.50
O2	8b	0.5	0.5	0.226(2)	0.0814(4)	0.39
O3	8b	0.5	0.5	0.238(1)	0.4236(5)	0.30
O4	8b	0.5	0.0	0.266(2)	0.0876(7)	0.36
O5	8b	0.5	0.0	0.276(2)	0.4168(7)	0.45
Zn	4a	0.25	0.5	0.5	0.12030(9)	0.44

[a] The isotropic equivalent thermal parameter is defined as $B = 4/3 [a^2\beta_{11} + b^2\beta_{22} + c^3\beta_{33} + 2ab(\cos\gamma)\beta_{12} + 2ac(\cos\beta)\beta_{13} + 2bc(\cos\alpha)\beta_{23}]$.

$ZnMo_8O_{10}$. In the initial stage of refinement, isotropic thermal parameters were assumed, and all the positional parameters for Mo atoms were assigned initial values equal to $LiMo_8O_{10}$. The remaining atoms were located from successive ΔF maps. The structure was then refined with anisotropic thermal parameters for all atoms except O4 and with an isotropic extinction parameter which yield final $R = 2.6\%$ and $R_w = 3.2\%$. The value for the secondary extinction parameter was 2.91×10^{-4}. A refinement including the multiplier for the zinc atom gave $m(Zn) = 0.251(2)$ indicating that the zinc site was fully loaded. A negative temperature factor was obtained for O4 when it was anisotropically refined. A difference-Fourier map calculated from the final refinement showed the maximum residual electron density of 0.8 e/Å^3 near Mo2. The final positional and isotropic thermal parameters are given in Table V. The selected bond distances and bond angles are listed in Tables VI and VII.

TABLE VI

BOND DISTANCES (Å) FOR $ZnMo_8O_{10}$

Mo1–Mo1	2.585(2)	Mo1–O1	2.197(6)
Mo1–Mo2	2.9525(2)	Mo1–O2	2.023(9)
Mo1–Mo3	2.836(1)	Mo1–O5	2.068(2)
Mo1–Mo4	2.760(1)	Mo2–O1	2.154(6)
Mo2–Mo2	2.817(2)	Mo2–O3	2.01(1)
Mo2–Mo3	2.680(1)	Mo2–O4	2.07(2)
Mo2–Mo4	2.734(1)	Mo3–O2	2.085(6)
Mo3–Mo3	2.694(2)	Mo3–O4	2.080(7)
	3.202(2)	Mo3–O5	2.19(2)
Mo4–Mo4	2.651(2)	Mo4–O3	2.037(6)
	3.245(2)	Mo4–O4	2.21(2)
Mo3–Mo4[a]	3.223(1)	Mo4–O5	2.108(6)
Mo1–Mo1[a]	3.311(2)	Zn–O2	1.881(9)
Mo2–Mo2[a]	3.079(2)	Zn–O3	1.93(1)

[a] Interchain distance.

Description of the Crystal Structures

General features. The most prominent structural feature of these compounds MMo_8O_{10} (M = Li or Zn) is the presence of infinite chains composed of edge-shared octahedral cluster units, as shown in Fig. 1. The individual chains are interlinked in the *ab* plane by Mo(w)—O—Mo(w) bonding to form layers (Mo(w) indicates waist atoms Mo1 and Mo2 along the chains). In the stacking of these layers along the *c* axis the

TABLE VII

BOND ANGLES (DEGREE) FOR $ZnMo_8O_{10}$[a]

Mo1–Mo1–Mo2	92.25(2)	O1–Mo1–O1	82.0(4)
Mo2–Mo1–Mo2	173.73(4)[b]	O1–Mo1–O2	86.7(5)
Mo1–Mo2–Mo2	87.75(2)	O1–Mo1–O5	91.8(5)
Mo4–Mo1–Mo1	62.08(2)	O2–Mo1–O5	178.0(4)
Mo4–Mo2–Mo2	58.99(2)	O1–Mo2–O1	88.8(3)
Mo3–Mo1–Mo1	62.89(2)	O1–Mo2–O3	86.7(5)
Mo3–Mo2–Mo2	58.30(2)	O1–Mo2–O4	87.3(5)
Mo4–Mo1–Mo2	57.08(3)	O3–Mo2–O4	171.7(3)
Mo3–Mo1–Mo2	55.12(3)	O2–Mo3–O2	79.5(4)
Mo1–O1–Mo2	85.45(3)	O2–Mo3–O4	90.6(3)
Mo2–O4–Mo4	177.0(5)	O2–Mo3–O4	167.4(4)
Mo3–O4–Mo4	97.3(5)	O2–Mo3–O5	88.5(3)
Mo1–O5–Mo3	179.8(5)	O4–Mo3–O4	97.9(3)
Mo3–O5–Mo4	97.1(5)	O4–Mo3–O5	83.4(5)
O2–Zn–O2	118.2(6)	O3–Mo4–O3	98.6(3)
O2–Zn–O3	110.6(2)	O3–Mo4–O4	88.7(4)
O3–Zn–O3	93.3(6)	O3–Mo4–O5	91.2(2)
		O3–Mo4–O5	166.5(4)
		O4–Mo4–O5	82.2(5)
		O5–Mo4–O5	77.8(4)

[a] The atom labels refer to Fig. 2.

[b] This angle corresponds to the dihedral angle between basal planes of adjacent octahedra.

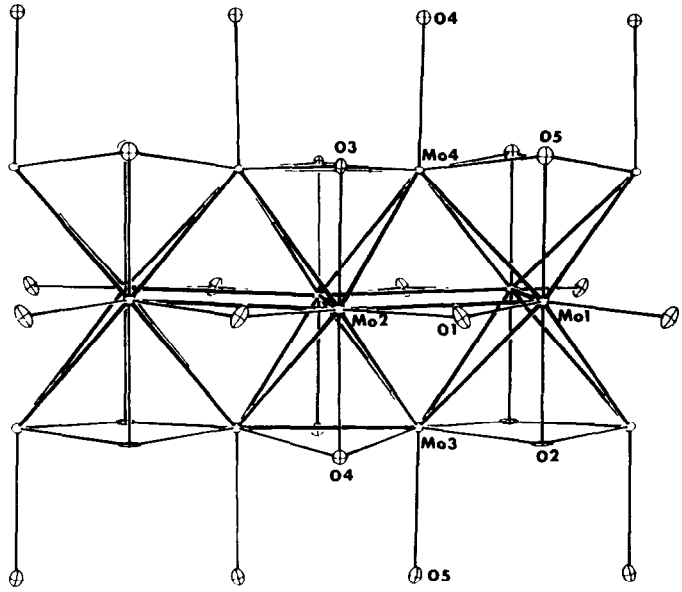

FIG. 1. A section of one molybdenum oxide cluster chain in MMo$_8$O$_{10}$ (M = Li or Zn). Mirror planes perpendicular to the chain axes contain the edge-shared bonds located at Mo1 and Mo2. Atoms Mo3, Mo4, O4, and O5 are contained in a mirror plane parallel to the chain axes.

infinite chains are directed alternately along the a and b axes in successive layers, as shown in Fig. 2. The infinite chains in one layer are bound to those in layers above and below by Mo(a)—O—Mo(a) crosslinking (Mo(a) indicates apical atoms Mo3 and Mo4 along the chains). Sharing of atoms between cluster units within a chain and between chains is indicated by the connective formula (5) $[(Mo_2Mo_{4/2}O^{i-i}_{6/2}O^{i-a}_{4/3})O^{a-i}_{2/3}]$ for the Mo_4O_5 subunit. Mirror planes perpendicular to the chain axis pass through the shared cube faces defined by atoms Mo1, O2, O2′, O5, O5′ and Mo2, O3, O3′, O4, O4′. Symmetry-related mirror planes thus also contain the chain axis and atoms O4, Mo4, Mo3, O5. The true crystallographic repeat unit then contains two edge-shared octahedral cluster subunits. Because there is no mirror or glide plane relating Mo3 to Mo4 or Mo1 to Mo2, the bonding within these octahedral subunits is far less regular then in the compounds $M^tM^oMo_4O_7$ (2) which also contain two edge-shared octahedral cluster subunits in the true chain repeat unit. The latter, however, contain a glide plane which relates apical-to-apical, and waist-to-waist atoms along each chain.

If one regards the infinite chain as a rectangular column, then the observed structure can be regarded as a crosswise stacking of these columns perpendicular to the c axis as represented in Fig. 2. In the unit cell there are four layers of columns with z values of $\frac{1}{8}$, $\frac{3}{8}$, $\frac{5}{8}$, and $\frac{7}{8}$ required by the body-centered structure. This arrangement can be described in the idealized space group $I4_1/amd$ if the lack of the above-mentioned glide plane is disregarded. Some of the symmetry elements for the latter space group are shown in Fig. 3. The structure of these compounds MMo$_8$O$_{10}$ can be related to that of the compounds $M^tM^oMo_4O_7$ (orthorhombic, space group *Imma*) by substitution of single metal atom chains (M^oO_2) for Mo_4O_5 cluster chains in alternate layers

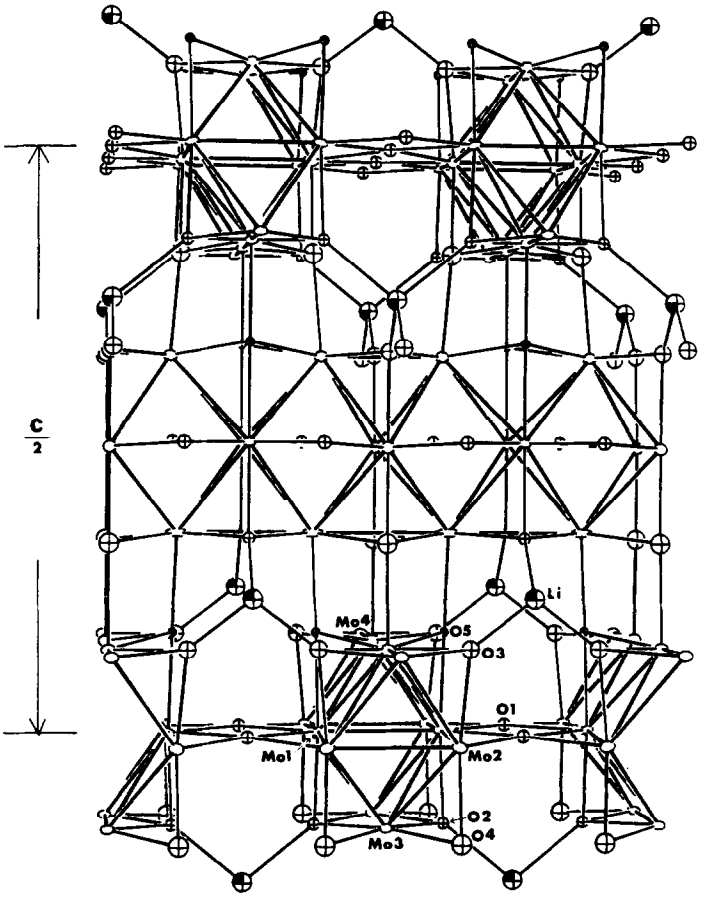

FIG. 2. A section of the structure of $LiMo_8O_{10}$ as viewed down the tetragonal a axis. Open ellipsoids are Mo, crossed spheres O, and shaded spheres Li.

of the crosswise stacking pattern. This analogy is emphasized by the formulations $M^t(M^oO_2)(Mo_4O_5)$ and $M^t(Mo_4O_5)(Mo_4O_5)$ for the two structures, where M^t and M^o indicate ternary metal ions in tetrahedral and octahedral coordination sites, respectively.

It is interesting that each of the above structures is related to the cubic spinel structure $M^tM^o_2O_4$, space group $Fd3m$. If one elongates the spinel structure along one crystallographic axis, a derivative structure is obtained which contains chains of metal atoms M^o in the octahedral coordination sites running along the cubic [110] and [1$\bar{1}$0] directions. With conventional choice of axes the new unit cell belongs to space group $I4_1/amd$, a tetragonal subgroup of $Fd3m$, as shown in Fig. 4. Substitution of the M^oO_2 chains by Mo_4O_5 cluster chains results in the structure of $M^tMo_8O_{10}$, emphasized by the related formulations $M^t(M^oO_2)_2$ and $M^t(Mo_4O_5)_2$. Substitution of Mo_4O_5 cluster chains only in alternate layers of the spinel structure gives the orthorhombic subgroup $Imma$ and the compounds $M^t(M^oO_2)(Mo_4O_5)(M^tM^oMo_4O_7)$, with the M^oO_2 chains oriented along the a axis, and the Mo_4O_5 chains along the b axis. Thus, just as the spinel structure can be

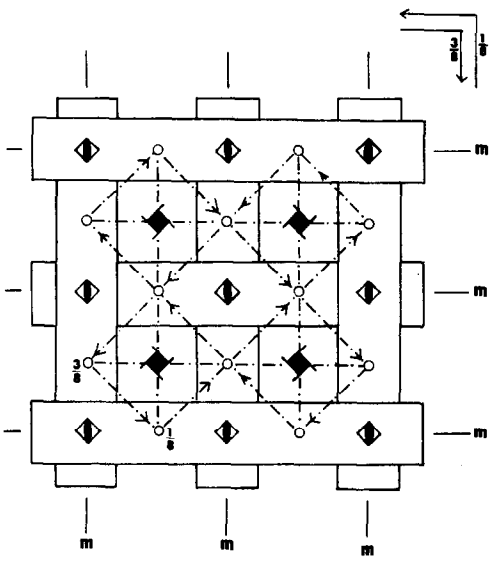

FIG. 3. A projection of the M Mo$_8$O$_{10}$ structure along the tetragonal c axis showing the molybdenum oxide chains represented as rectangular columns. Positions and directions of the symmetry elements for the idealized space group $I4_1/amd$ are indicated.

regarded as an ordered-defect NaCl structure (disregarding the M^t atoms in tetrahedral coordination sites), so also can the structures of M^tMo$_8$O$_{10}$ and M^tM^oMo$_4$O$_7$ be viewed in this way. Related compounds having ordered-defect NaCl structures which result in metal–metal bonding are TiO and NbO (*10*). In particular, the defect ordering in NbO results in apex-shared octahedral cluster units $Nb_{6/2}O_{12/4}$ forming infinite chains parallel to the three cubic axes. In this case each cluster is a member of three intersecting chains.

Metal–metal bonding. The Mo—Mo bonding within the octahedral cluster units is quite distorted compared to the regular bonding pattern in NaMo$_4$O$_6$ (*1*). Whereas all apex–apex and waist–waist bond distances are equal along the chains of Na Mo$_4$O$_6$, these are alternately short and long for LiMo$_8$O$_{10}$ and ZnMo$_8$O$_{10}$. As shown in Fig. 5 the pattern of apex–apex distances is slightly different for LiMo$_8$O$_{10}$ than for Zn Mo$_8$O$_{10}$. In the Li compound when the apex–apex distance is short on one side of the chain it is long on the other side, while in the Zn compound this distance is either short or long at equal positions on both sides of the chain. The short distances of 2.62 to 2.69 Å represent strong pairwise coupling of the apex Mo atoms with a Mo—Mo bond order of close to unity. Pairwise coupling of the apex atoms is also found in compounds with the Sc$_{0.75}$Zn$_{1.25}$ Mo$_4$O$_7$ structure (*2*). In these cases metal-centered electron counts (MCE) (*18*)

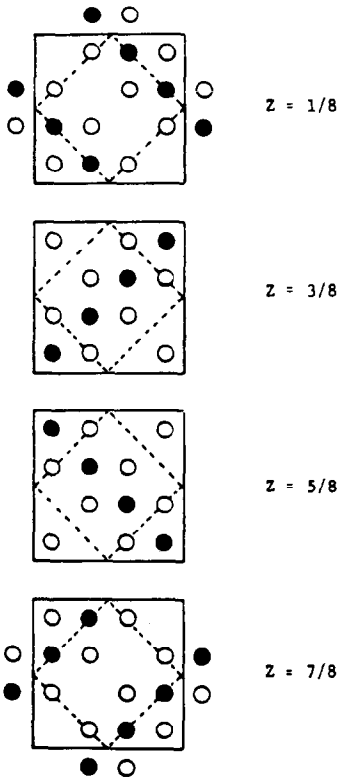

FIG. 4. A schematic representation of the spinel structure projected on (001). The four panels show successive layers of the structure. The filled and open circles represent octahedral metal and oxygen atoms, respectively. The tetrahedrally coordinated metal atoms in the spinel structure $M^tM^o_2O_4$ are not shown. A smaller unit cell for the tetragonal space group $I4_1/amd$ is indicated by the dashed lines.

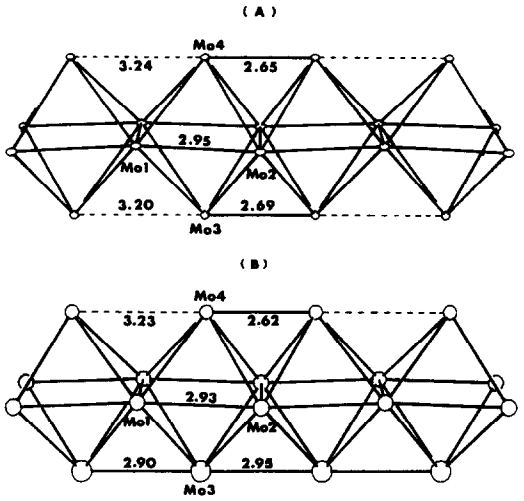

FIG. 5. Sections of the octahedral cluster chains in (A) $ZnMo_8O_{10}$ and (B) $LiMo_8O_{10}$. Only the bonds between Mo atoms are shown.

in the Mo_4 repeat units are all in the range 14.5–15.0, while in $NaMo_4O_6$ with equal apex–apex spacings, MCE = 13.0. As noted elsewhere (*18*), the pairwise distortion along the chains appears to be driven by the higher MCE count. In effect, for MCE > 13, continued addition of electrons causes distortions from the regular bonding in the cluster units so as to avoid occupation of antibonding states. The total Mo—Mo bond order,[2] summed over all Mo—Mo bonds of the repeat unit, is thus greater for these distorted units than for the undistorted units in $NaMo_4O_6$ (*18*). For example, these Mo—Mo bond order sums show increasing values of 6.35, 6.85, and 7.05 for the Mo_4 units in $NaMo_4O_6$, $LiMo_8O_{10}$, and $ZnMo_8O_{10}$, respectively, even though the average Mo—Mo bond distance (averaged over all Mo—Mo bonds of the octahedral subunits) remains essentially constant (2.803, 2.800, and 2.809 Å, respectively).

The cause for the different pattern of apex–apex pairings in $LiMo_8O_{10}$ vs those in $ZnMo_8O_{10}$ is difficult to assess. It is possible that the greater MCE of 15 for the latter, as opposed to 14.5 for the former, may be responsible for this difference. However the interplay of Mo—O and Li—O or Zn—O bonding may also contribute to this effect. In $LiMo_8O_{10}$ we note that d(Li—O3) < d(Li—O2), whereas in $ZnMo_8O_{10}$, d(Zn—O3) > d(Zn—O2). This reversal in the order of corresponding distance is transmitted to the Mo—O bonding where in $LiMo_8O_{10}$, d(Mo4—O3) > d(Mo3—O2), but in $ZnMo_8O_{10}$, d(Mo4—O3) < d(Mo3—O2). Thus in $ZnMo_8O_{10}$, d(Mo3—O2) = 2.085(6) Å, and in $LiMo_8O_{10}$ the corresponding distance is 2.015(8) Å. In turn we find that the Mo3—Mo3 bond bridged by O2 is shorter, 2.694(2) Å, for $ZnMo_8O_{10}$ than for $LiMo_8O_{10}$, 2.950(3) Å. Evidently, weakening of the Mo3—O2 bond in $ZnMo_8O_{10}$ permits a strengthening of the Mo3—Mo3 bond bridged by O2. Whether the difference in MCE counts or effects arising from the difference in M—O (M = Li or Zn) bonding is more important in bringing about this interesting structural difference between $LiMo_8O_{10}$ and $ZnMo_8O_{10}$ cannot be decided.

Another noteworthy feature of the Mo—Mo bonding in both of these compounds is the alternating lengths of the bonds between waist atoms on the shared edges of the octahedral cluster units. The Mo1—Mo1 distances are 2.648(2) and 2.585(2) Å, respectively, for $LiMo_8O_{10}$ and $ZnMo_8O_{10}$, while the Mo2—Mo2 distances are 2.754(3) and 2.817(2) Å, respectively. Perhaps this feature is most striking because of the very short Mo1—Mo1 distance of 2.585 Å in $ZnMo_8O_{10}$. By comparison with the distance 2.614 Å, which has been established as a very acceptable value for the Mo—Mo single bond distance in com-

[2] Individual Mo—Mo bond orders (n) are calculated from the Pauling equation relating bond distance to bond order, $d(n) = d(1) - 0.6 \log n$, where $d(n)$ is the observed bond distance in Ångstroms, $d(1)$ is the distance for a bond of order $n = 1$ (for Mo $d(1) = 2.614$ Å). L. Pauling, "Nature of the Chemical Bond," 3rd ed., p. 400, Cornell Univ. Press, Ithaca, N.Y., 1960.

pounds containing these octahedral cluster chains (*18*), the 2.585-Å distance indicates multiple bond character. The possibility of both σ and π contributions to the *M*—*M* bonds between metal atoms on the shared edges of the units in these chains has recently been demonstrated by the band calculations of Bullett (*19*). Again this behavior emphasizes the point that with increasing MCE count beyond about 13*e*/ unit, the bonding within the repeat units becomes more irregular. Apparently increasing electron concentration favors localization of electrons by pairwise (two-center) bonding, especially apex–apex and waist–waist pairing, where the latter occurs perpendicular to the chain axis. This result is also observed in the remarkable new compound $In_{11}Mo_{40}O_{62}$, which contains discrete cluster units $Mo_{18}O_{28}$ and $Mo_{22}O_{34}$, consisting of four and five edge-shared octahedral cluster subunits, respectively (*20*). More extensive examination of these systems by band structure calculations is needed to provide additional insight about the relation between electron concentration and the pairwise distortions within the cluster units.

Metal–oxygen bonding. The five crystallographically different O atoms can be grouped into three distinct types according to their coordination geometries, as can be discerned from Fig. 2. Atoms O2 and O3 are pseudotetrahedral, each bonded to three Mo and one ternary metal atom (Li or Zn). The intralayer, interchain bridging atoms O1 are coordinated by four waist Mo atoms (Mo1 and Mo2) in approximate square-planar symmetry. Atoms O4 and O5 are each bonded to two apex and one waist Mo atom within one chain and one apex Mo in a neighboring chain in a geometry like the bond configuration about the sulfur atom in SF_4. In fact, while these latter two bond configurations about O atoms are unusual, they are also evident in other compounds containing octahedral cluster chains, e.g., $Mn_{1.5}Mo_8O_{11}$ (*3*), $Sc_{0.75}Zn_{1.25}Mo_4O_7$ (*2*), and NbO (*10*). Notably these bond configurations are generated in the ordered-defect NaCl structures when vacancies are present in two of the six metal atom positions surrounding an O atom.

The tetracoordinated ternary metal cations are located on 4*a* special positions and have local symmetry of C_{2v}. There are thus two different *M*—O bond distances, and all are somewhat shorter than the predicted value (1.98 Å) using the effective ionic radii of Shannon (*21*). The Li—O3 distance of 1.70 Å is unusually short, and the average Li—O distance of 1.83 Å appears to place the Li^+ ion under unusual compression. As noted in the Synthesis section attempts to prepare isomorphous compounds containing other small cations (Mg, Fe, Co, Ni, Si), known to readily accept tetrahedral coordination, were unsuccessful.

Note added in proof. Tables of anisotropic temperature factors and structure factors: see NAPS Document No. 04396 for 5 pages of supplementary materials from ASIS/NAPS, Microfiche Publications, P.O. Box 3513, Grand Central Station, New York, New York 10163. Remit in advance $4.00 for microfiche copy or for photocopy, $7.75 up to 20 pages plus $.30 for each additional page. All orders must be prepaid.

References

1. C. C. Torardi and R. E. McCarley, *J. Amer. Chem. Soc.* **101,** 3963 (1979).
2. R. E. McCarley, *ACS Symp. Ser.* **211,** 273 (1983); *Philos. Trans. R. Soc. London Ser. A* **308,** 141 (1982).
3. C. D. Carlson, P. A. Edwards, and R. E. McCarley, to be published.
4. R. E. McCarley, K.-H. Lii, P. A. Edwards, and L. F. Brough, *J. Solid State Chem.* **57,** 17 (1985).
5. A. Simon, *Chem. Unserer Zeit* **10,** 1 (1976).
6. J. D. Corbett and R. E. McCarley, *in* "Crystal Chemistry and Properties of Materials with Quasi-One-Dimensional Structure" (J. Rouxel, Ed.), pp. 179–204, Reidel, Dordrecht, Holland (1985).
7. C. C. Torardi and R. E. McCarley, *Inorg. Chem.* **24,** 476 (1985), and references therein.

8. C. C. TORARDI AND R. E. MCCARLEY, *J. Solid State Chem.* **37,** 393 (1981).

9. C. C. TORARDI AND J. C. CALABRESE, *Inorg. Chem.* **23,** 3281 (1984).

10. J. K. BURDETT AND T. HUGHBANKS, *J. Amer. Chem. Soc.* **106,** 3101 (1984), and references therein.

11. K. B. SCHWARTZ, C. T. PREWITT, R. D. SHANNON, L. M., CORLISS, J. M. HASTINGS, AND B. CHAMBERLAND, *Acta Crystallogr. Sect. B* **38,** 363 (1982).

12. D. CAHEN, J. A. IBERS, AND J. B. WAGNER, JR., *Inorg. Chem.* **13,** 1377 (1974).

13. I. D. BROWN, B. D. CUTFORTH, C. G. DAVIES, R. J. GILLESPIE, P. R. IRELAND, AND J. E. VEKRIS, *Canad. J. Chem.* **52,** 791 (1974).

14. K.-H. LII, F. DISALVO AND R. E. MCCARLEY, to be published.

15. R. A. JACOBSON, *J. Appl. Crystallogr.* **9,** 115 (1976).

16. H. P. HANSON, F. HERMAN, J. D. LEA, AND S. SKILLMAN, *Acta Crystallogr.* **17,** 1040 (1964).

17. D. H. TEMPLETON, *in* "International Tables for X-Ray Crystallography" (C. H. Macgillavry and G. D. Rieck, Eds.), 1st ed., Vol. III, p. 215, Kynoch Press, Birmingham (1962).

18. R. E. MCCARLEY, *Polyhedron* **5,** 51 (1986).

19. D. W. BULLETT, *Inorg. Chem.* **24,** 3319 (1985).

20. H.-J. MATTAUSCH, A. SIMON, AND E.-M. PETERS, *Inorg. Chem.*, in press.

21. R. D. SHANNON, *Acta Crystallogr. Sect. A* **32,** 751 (1976).